INVESTIGATION OF Te DOPED ZnO SYNTHESIZED BY SOL-GEL TECHNIQUE

Eyüp Fahri KESKENLER[1]*, Güven TURGUT[2], Mustafa Furkan KESKENLER[3]

[1] *Recep Tayyip Erdoğan University, Faculty of Engineering, Department of Material Science and Nanotechonology, 53100 Rize, Turkey*

[2] *Erzurum Technical University, Faculty of Basic Sciences, Department of Physics, 25240 Erzurum, Turkey*

[3] *Atatürk University, Faculty of Engineering, Department of Computer Engineering, 25240 Erzurum, Turkey*

Abstract: In this study, structural, morphological and optical properties of Te doped ZnO thin films prepared by sol-gel spin coating method were investigated. It was observed that the hexagonal wurtzite structure of ZnO for all samples and cubic zinc blende structure of ZnTe for 3 and 5 % at. Te doped ZnO films. The obtained films exhibited wurtzite (002) preferential growth in all the dopant ratios. Grain size values calculated from Scherrer's formula of the films were varied in range of 107-188 nm. The band gap energy values were determined as 3.352, 3.292, 3.272, 3.248, 3.156 eV, respectively for undoped ZnO, 1%, 2%, 3%, 5% at. Te doped ZnO samples. Also, Urbach energy values of samples were found to be 2.07, 1.72, 1.34, 1.32, 0.97 eV for undoped ZnO, 1, 2, 3 and 5 at. % Te doped ZnO, respectively.

Keywords: ZnO, Te, Sol-Gel, Urbach Rule, Steepness Parameters

*Corresponding author: Recep Tayyip Erdoğan University, Faculty of Engineering, Department of Material Science and Nanotechonology, 53100 Rize, Turkey
Email: keskenler@gmail.com (E. F. KESKENLER)

1. Introduction

Zinc oxide (ZnO) has many potential applications in light-emitting diodes, laser diodes, photo- detectors (Jiang et al., 2009; Lee et al., 2011), varistors, sensors, piezoelectric nano-generators, thin film solar cells, flat panel and liquid crystal displays (Pawar et al., 2008; Sanchez-Juarez, Tiburcio-Silver, Ortizc, Zironi, and Rickards, 1998) due to its unique properties such as relatively low cost, abundance in nature, easy fabrication, non-toxicity, low electrical resistivity, good optical transparency in the visible region direct energy band gap with a large excitation binding energy of 60 meV (Chouikh et al., 2011; Pawar et al., 2008; Sanchez-

Juarez et al., 1998) high chemical stability under reducing atmosphere(Biswal et al., 2010). ZnO is generally an n-type wide-gap semiconductor due to the lack of stoichiometry resulting mainly from oxygen vacancies (Iribarren et al., 2008a). These vacancies induce the formation of deep trap levels into band gap (Iribarren, Fernández, and Piqueras, 2009b).Doping of isovalent impurities in II-VI compounds allows to tailor physico-chemical characteristics of ZnO such as structural, morphological, optical, electrical, and magnetic (Karthikeyan et al., 2009; Wenckstern et al., 2009). Te which is one of isovalent impurities,can considered to act as an isoelectronic donor judging

from its much lower electron affinity compared with O(S. Park et al., 2010; S. H. Park et al., 2010). Particularly, the band gap of ZnO can be adjustedwith diffusion of Te into ZnO films (Iribarren et al., 2008b, Iribarren et al., 2009a; Iribarren et al., 2009b). When Te diffuse into ZnO, the structure of $ZnO_{1-x}Te_x$ forms and the band gap of $ZnO_{1-x}Te_x$ varies from about 2.39 eV (for x=1) and 3.44 eV (for x=0) according to value of x (Merita et al., 2004; Wenckstern et al., 2009).In earlier studies, Te or N and Te co-doped ZnO structures have been grown by vapour–solid process (Iribarren et al., 2008a), plasma-assisted molecular beam epitaxy (P-MBE)(S. Park et al., 2010), metal-organic chemical vapordeposition process (Tang et al., 2010), pulsed laser deposition (Porter and Muth, 2006). The sol-gel spin coating technique is attractive due to its easy manipulation of the samples, ability to prepare high quality thin films in large scale, safety, low cost of apparatus (Ghodsi and Absalan, 2010), deposition of high purity (Roknabadi, Behdani, Arabshahi, and Hodeini, 2009; Sagar, Kumar, and Mehra, 2005), easy control of chemical components (Ilıcan et al., 2008).

Therefore, we aimed to investigate that Te doping effect on the structural, morphological and optical properties of ZnO thin films.

2. Experimental

In the present work, undoped and Te doped ZnO at different Te concentrations thin films were deposited on microscopic glass substrates by spin coating sol-gel method. The coating precursor solution was prepared by using zinc acetate dehydrate [$Zn(CH_3COO)_2.2H_2O$] as a starting material together with 2-Methoxyethanol ($C_3H_8O_2$) and monoethanolamine (C_2H_7NO, MEA) werea solvent and stabilizer, respectively. For Te doping solution, the tellurium tetrachloride ($TeCl_4$) was inserted into the solution to use as the tellurium source. The molar ratios of $Zn(CH_3COO)_2.2H_2O$ to MEA were maintained at 1:1. 0.5 M Zinc acetate dehydrate and 0.5 M tellurium tetrachloride were mixed in different solution atomic percent ratios; 0 at, 1at, 2 at, 3 at, 5 at. %. The sol solutions were stirred at 70 °C for 8 h to obtain a clear and homogenous solution. The glass substrates the firstly were kept in boiling chromic acid solution and then they were rinsed with deionized water. Finally, they were cleaned acetone, deionized water and methanol by using an ultrasonic cleaner and dried with nitrogen.

In the spin coating process, the resultant solution was dropped on glass substrate, which was rotated at a speed of 2500 rpm for 20 sec by using a spin-coater. The as-coated film was sintered at 200 °C for 5 min to evaporate solvent and remove the organic sediments and then spontaneously cooled to room temperature. This procedure was repeated for 7 times to obtain the intended thickness and film quality. The same procedure was repeated for the films prepared with different values of Te doped and finally, they were annealed in air at 400oCfor 30 minutes.

In addition X-ray diffraction (XRD) patterns were taken using a Rigaku Miniflex II diffractometer. The diffractometer reflections were investigated at room temperature and the values of 2θ were altered between 15o and 90o. The incident wavelength was 1.5418 Å. The optical absorbance of the thin films were recorded in spectral region of 300-1000 nm at 300 K using a UV-VIS spectrophotometer (Perkin-Elmer, Lambda 40) which works in the range of 200-1100 nm and has a wavelength accuracy of better than ±0.3 nm.

3. Results and Discussion

3.1. Structural and morphological properties

The crystal structure and orientation of undoped and Te doped ZnO thin films were investigated by X-ray diffraction (XRD) patterns. Figure 1 showed the XRD patterns of undoped and Te doped zinc oxide films deposited at different Te dopant concentrations.
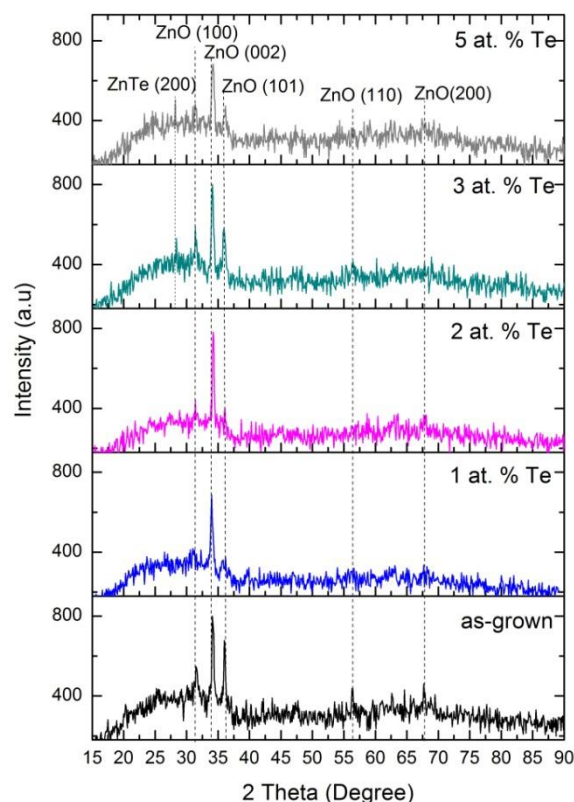
Figure 1. XRD pattens of 1, 2, 3, 5 at. % Te doped ZnO films.

These spectra indicated that the films had polycrystalline nature. ZnO hexagonal wurtzite structure (JCPDS card file no. 36-1451) with peak of

(100), (002), (101), (110), (200) was observed for undoped sample. The peaks of (110), (200) were almost disappeared with Te doping. The most peak intensity was (002) for all samples. The highest peak intensity of (002) was also observed by Lee et al. (2003). When Te doping ratioswere3 and 5 at. %, the ZnTe cubic phase peak of (200) (JCPDS card file no: 15-0746) was emerged at low intensities. Namely, ZnO binary structure changed to ZnO1-xTex ternary structure with the increasing Te doping ratio. ZnO1-xTex ternary structures with Te doping were also observed by Tang et al. (2010) from XRD analysis. In addition to, these structures were observed by CL measurements (Iribarren et al., 2008b). The reason for small intensity or no intensity of ZnTe may be very small Te atomic concentration in ZnO structures. For these structures calculated interplanar distance 'd' values from XRD analysis were presented in Table 1 and these values were compared with the standard ones from JPDS card no: 36-1451 and JPDS card no: 15-0746.

Table 1. The structural parameters of Te doped ZnO thin films

Doping ratio (% at. Te)	(hkl)	$d_{calculated}$	$d_{standard}$	Lattice constants of ZnO		Lattice constant of ZnTe	D (nm)	δ(x 10^{13} lines/ m^2)
				a (a_{st}=3.249)	c (c_{st}=5.206)	a (a_{st}=6.103)		
0.0	ZnO 100)	2.8042	2.8143	3.246	5.172	-	188	2.84
	ZnO(002)	2.5859	2.6033					
	ZnO(101)	2.4698	2.4759					
	ZnO(110)	1.6031	1.6247					
	ZnO(200)	1.3990	1.4077					
1.0	ZnO(100)	2.8135	2.8143	3.250	5.211	-	156	4.09
	ZnO(002)	2.6057	2.6033					
	ZnO(101)	2.4762	2.4759					
2.0	ZnO(100)	2.8206	2.8143	3.257	5.222	-	135	5.47
	ZnO(002)	2.6112	2.6033					
	ZnO(101)	2.4819	2.4759					
3.0	ZnTe200)	3.0830	3.0510	3.262	5.239	6.166	118	7.18
	ZnO 100)	2.8151	2.8143					
	ZnO(002)	2.6196	2.6033					
	ZnO(101)	2.4862	2.4759					
5.0	ZnTe200)	3.1433	3.0510	3.276	5.244	6.287	107	8.77
	ZnO(100)	2.8336	2.8143					
	ZnO(002)	2.6221	2.6033					
	ZnO(101)	2.4950	2.4759					

The lattice constants 'a' and 'c' of the wurtzite structure of ZnO and lattice constant 'a' of the cubic ZnTe were calculated using the relations (Bowen et al., 2011; Tilley, 2006);

$$\frac{1}{d^2} = \frac{4}{3}\left(\frac{h^2+k^2+hk}{a^2}\right)+\left(\frac{l^2}{c^2}\right)$$

$$\frac{1}{d^2} = \left(\frac{h^2+k^2+l^2}{a^2}\right)$$

where 'd' is the interplaner distance and (hkl) miller indices, respectively. The standard and calculated lattice constants were given in Table 1. For ZnO, these values agree with ones from JPDS card no: 36-1451 and they slightly increased with increasing Te doping ratio. The formation of ZnTe may increase lattice constants due to the size of Te bigger O (Iribarren et al., 2009a, 2009b; Park et al., 2010). But lattice constants of ZnTe are slightly bigger than standard one (JCPDS card no: 15-0746). From linear Vegard's law (Denton and Ashcroft, 1991) and given the c lattice constants of w-

ZnTe 0.7090 nm (JCPDS card no: 19-1482), and w-ZnO 0.5206 nm (JCPDS card no: 36-1451), the atomic concentration of Te in solid ZnTexO1−x were estimated to be x=0.265%, 0.849 %, 2.77 % and 3.19 % for 1, 2, 3, and 5 % at. Te doped samples, respectively. These atomic ratios for ZnTexO1−x alloys were smaller than ones in solutions. It probably could be with much smaller Te incorporation rate in solidthan in gas phase (Tang et al., 2010).

For peak of (002), the average crystallite sizes of the films were calculated by using Scherrer's formula (Scherrer and Nachrichten, 1918);

$$D = \frac{0.9\lambda}{\beta\cos\theta}$$

where D was the crystallite size, wavelength of the X-ray used was λ =1.5418 Å, β was the broadening of diffraction line measured at the half of its maximum intensity in radians and θ was the angle of diffraction. The values of calculated average grain size were given in Table 1. As seen from Table 1, the grain size value of

undoped sample continuously decreased from 188 nm to 107 nm with increasing Te doping content. The dislocation density (δ), defined as the length of dislocation lines per unit volume (lines /m2) and the dislocation density (δ) is the measure of the amount of the defects in a crystal. The dislocation density (δ) of samples was estimated using the equation (Ravichandran et al., 2009),

$$\delta = 1/D^2$$

The calculated dislocation density values (δ) showed increasing tendency with increasing Te content.

The surface morphology and thickness of the films were investigated with scanning electron microscope. The film thickness was estimated about to be 670 nm for the films by cross-section SEM images (in Figure 2.a). From the results of SEM analysis shown in Figure 2 (b-f), it was quite clear nanoparticles at surface of the films and the surface nature of the films was greatly affected by the variation of Te dopant concentration.

This particle-like structure was similar to the Chen at al. (2009) and Chakraborty at al. (2008). In addition, it can be seen that Te doping to ZnO structure increased particle size of undoped ZnO film. These results compliances with ones calculated from Scherrer's formula. There are large lattice mismatches between ZnTe and ZnO due to the difference in the bond lengths of Zn–Te (0.2670 nm), Zn–O (0.2089 nm) induced lattice deformations(Sargolzaei, Lotfizadeh, and Hayn, 2011)and high dislocation density.

3.2. Optical properties

Optical transmission spectra of doped and undoped samples were recorded in the wavelength range 300–1000 nm and were drawn in Figure 3. From transmittance spectra, there was reduction continuously with Te doping at all wavelength ranges. The optical transmission shifted red with increasing tellurium content. Namely, the transmittance in the short wavelengths showed decreasing tendency with increasing Te concentration. The decreasing transmittance with isovalent dopants were observed by Pan et al. (2010). The absorption coefficient (α) of the films was determined by the equation (Serin et al., 2006),

$$\alpha = \ln(1/T)/d$$

where T is transmittance and d is film thickness. The optical band gap was obtained by following relation (Tauc, Grigorovici, and Vancu, 1966),

$$\alpha h\nu = A(h\nu - E_g)^{1/2}$$

according to the relationship equation, where hν and Awere photon energy and the constant, respectively.
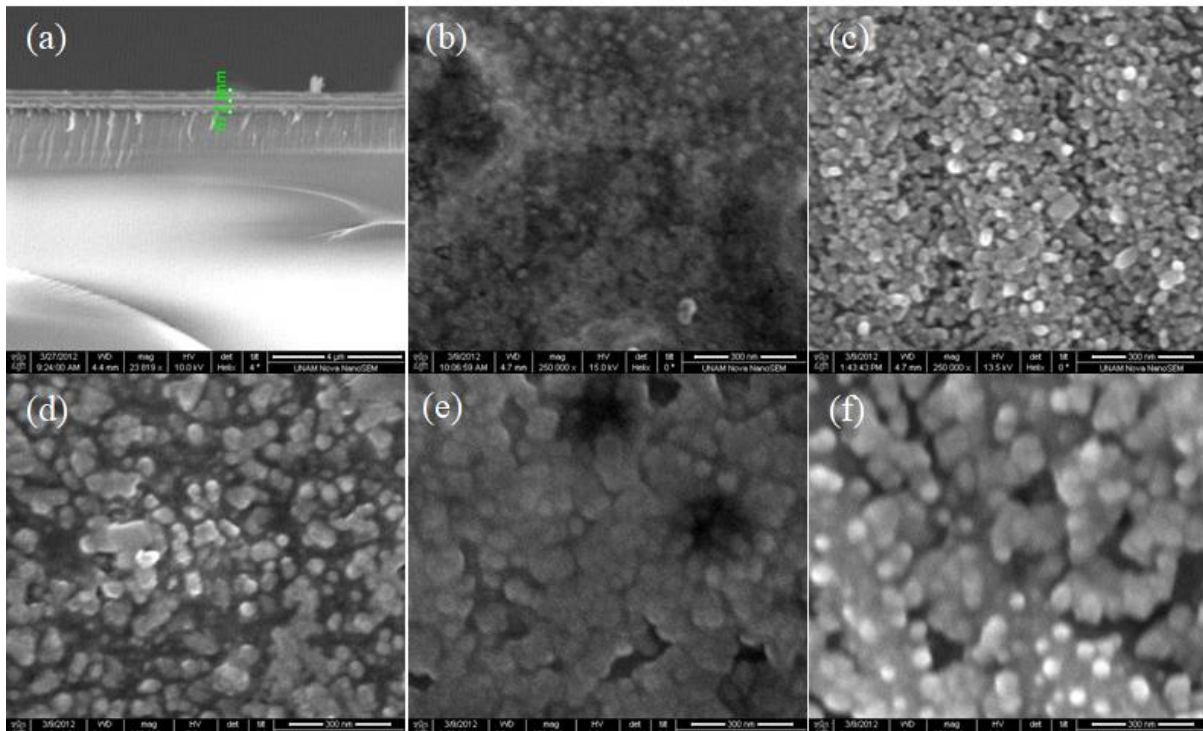
Figure 2. SEM images of Te doped ZnO films (a) cross-section of 2 at. % Te doped samples (b) undoped ZnO (c) 1 at. % doped ZnO (d) 2 at. % doped ZnO (e) 3 at. % doped ZnO (f) 5 at. % Te doped ZnO
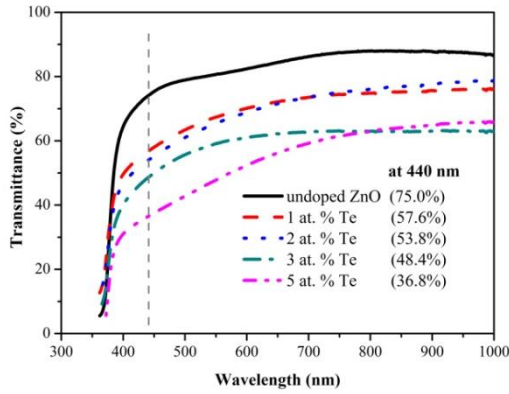
Figure 3. Transmittance spectra of Te doped ZnO films

From Figure 4, Eg values were determined by plotting $(\alpha h\nu))^2=0$ vs. $h\nu$ and extrapolating of the linear region of the plot to zero absorption $((\alpha h\nu)^2=0)$. The band gap values of undoped, 1, 2, 3 and 5 at. % Te doped ZnO thin films were found as 3.352, 3.292, 3.272, 3.248, 3.156 eV, respectively. In this study, when Te doping concentration is increased, $ZnO_{1-x}Te_x$ alloys formed. For $ZnO_{1-x}Te_x$, when x is increased up to about 0.7, the band gap of $ZnO_{1-x}Te_x$ continuously decreased to about 2 eV (Maksimov, 2010; Wenckstern et al., 2009). In this study, E_g values decreased to 3.156 eV due to x value varied between 0.00265 and 0.0319. Also, relation between E_g and x in present study was compatible with studies in literature (Maksimov, 2010; Wenckstern et al., 2009). This situation suggested that whenTeCl$_4$ salts was used in the sol solution, then Te incorporation into the ZnO matrix in the oxygen sites increases and passivates the O vacancies. Te in O vacancies sites forms ZnTe sub-units into the ZnO lattice and $ZnTe_xO_{1-x}$ units form (Iribarren et al., 2008a). The forming of $ZnTe_xO_{1-x}$ structure was suggested by XRD spectra.
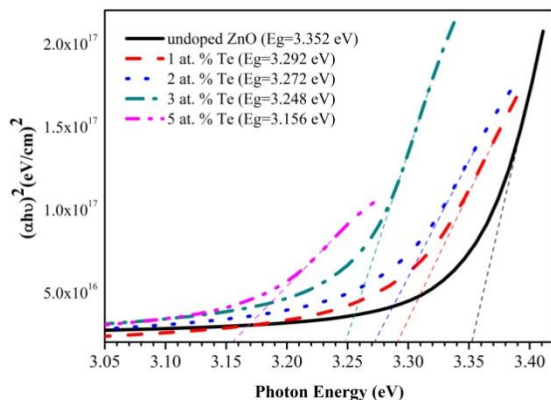
Figure 4. The variation of (⟦αhν⟧ ^2 vs. hν for Te doped ZnO samples

Exponential absorption tails for photon energies of sub-band gap both crystalline and amorphous materials have attracted considerable attention in recent years. However various mechanisms can be affected the absorption phenomena, the excitons have a significant role in it. The optical absorption coefficient shows a temperature-dependent exponential tail for E < Eg (Meulenkamp, 1999);

$$\alpha(E,T)=\alpha_0 \exp\left(\frac{E-E_0}{E_u(T,X)}\right) \qquad (1)$$

where, E_0 and α_0 are constants, which can be determined from the $\ln(\alpha)$ versus E obtained at series of different temperatures. Urbach energy, Eu, is assigned the steepness of Urbach tail. It is a function of temperature and the degree of crystal disorder of the material. It has a significant role on the characteristic analysis of a semiconductor. The previous statements imply that the Urbach energy can be expressed into two components as temperature-dependent and temperature-independent term:

$E_u (T, X) = E_u (T) + E_u (X)$

The thermal disorder of the material is associated the temperature-dependent term, while the temperature-independent component related to its inherent structural disorder (Meulenkamp, 1999). σ is steepness parameter that is found as:

$\sigma = kT/E_u$

By taking the natural logarithm on both sides of Eq. (1):

$$\ln\alpha = \frac{E}{E_u}\left(\ln(\alpha_0)+\frac{E_0}{E_u}\right)$$

E_u is equal to the absorption edge energy width and inverse to the absorption edge slope value,

$$E_u^{-1}=d(\ln\alpha)/d(E)$$

E_u should depend only on the degree of structural disorders (lattice strains and dislocation densities), i.e. as a function of X, in a constant temperature. In the present study, we have studied the E_u as a function of disorder on the $ZnTe_xO_{1-x}$ crystal structures by depositing thin film crystal. Figure 5 shows the $(\ln\alpha)$ versus photon energy $(h\nu)$ graph, aiming for calculating the Urbach energy values of samples. As seen in Table 2, E_u values were found to be 2.07, 1.72, 1.34, 1.32, 0.97 eV steepness parameters have been calculated 0.013, 0.015, 0.019, 0.020, 0.027 for undoped ZnO, 1, 2, 3 and 5 at. % Te doped ZnO, respectively. The Eu values of the films decreased and σ values increased considerably with increasing of Te doping in the films and as strated in the XRD analysis, this phenomena can be attributed that Te atoms affect the crystal structures by interstitial or substitution in crystalline.
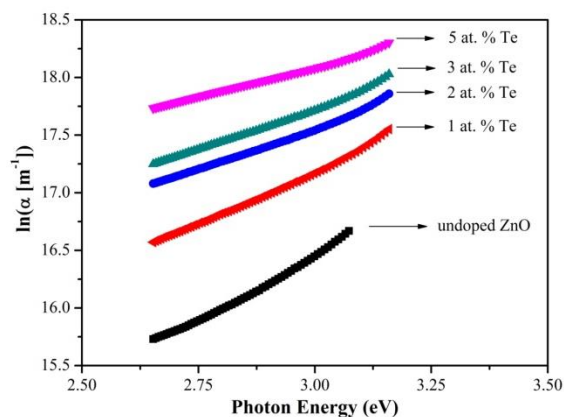
Figure 5. The variation of ln(α) vs. Photon energy for Te doped ZnO samples

Table 2. The optical band gap (Eg), Urbach energy (E_u) and steepness parameters (σ) values of Te doped ZnO thin films.

Sample	Eg (eV)	E_u (eV)	σ
0.0 at. % Te	3.352	2.07	0.013
1.0 at. % Te	3.292	1.72	0.015
2.0 at. % Te	3.272	1.34	0.019
3.0 at. % Te	3.248	1.32	0.020
5.0 at. % Te	3.156	0.97	0.027

4. Conclution

This paper presents Te doped ZnO thin films has been studied by sol-gel spin coating, using methanolamine, 2-methoxyethanol, zinc acetate dehydrate and tellurium tetrachloride for precursor solution.XRD studies indicated ZnO hexagonal wurtzite structure for all samples and ZnTe zinc blende structure for 3 and 5 % at. Te doped ZnO films. Grain sizes of the films were varied in range of 107-188 nm. SEM images of Te doped ZnO films showed the morphology and grain size and grain distribution of ZnO depend on Te dopant content. The band gap energy values were determined as 3.352, 3.292, 3.272, 3.248, 3.156 eV, respectively for undoped ZnO, 1%, 2%, 3%,5% at. Te doped ZnO samples. Also, Urbach energy and steepness parameters values of samples were found to be 2.07, 1.72, 1.34, 1.32, 0.97 eV and 0.013, 0.015, 0.019, 0.020, 0.027 for undoped ZnO, 1, 2, 3 and 5 at. % Te doped ZnO, respectively. Thus, Te doped ZnO thin films can be useful for many optoelectronic device applications.

References

Anonim 1994. FORTRAN Subroutines for Mathematical Applications. IMSL MATH/LIBRARY. Vol.1-2, Houston: Visual Numerics, Inc.

Biswal R R, Velumani S, Babu B J, Maldonado A, Tirado-Guerra S, Castaneda L, Olvera M D l L. 2010. Fluorine doped zinc oxide thin films deposited by chemical spray, starting from zinc pentanedionate and hydrofluoric acid: Effect of the aging time of the solution. Mat Sci Eng B, 174: 46-49.

Bowen A, Li J, Lewis J, Sivaramakrishnan K, Alford T L, Iyer S.

2011. The properties of radio frequency sputtered transparent and conducting ZnO: F films on polyethylene naphthalate substrate. Thin Solid Films, 519: 1809.

Chakraborty A, Mondal T, Bera S K, Sen S K, Ghosh R, Paul G K. 2008. Effects of aluminum and indium incorporation on the structural and optical properties of ZnO thin films synthesized by spray pyrolysis technique. Mat Chem Phy, 112: 162.

Chen K J, Hung F Y, Chang S J, Hu Z S. 2009. Microstructures, optical and electrical properties of In-doped ZnO thin films prepared by sol–gel method. Appl Surf Sci, 255: 6308.

Chouikh F, Beggah Y, Aida M S. 2011. Optical and electrical properties of Bi doped ZnO thin films deposited by ultrasonic spray pyrolysis. J Mater Sci: Mater Electron, 22: 499-505.

Denton A R, Ashcroft N W. 1991. Vegard's law. Physical Review A, 43: 3161-3164.

Ghodsi F E, Absalan H. 2010. Comparative Study of ZnO Thin Films Prepared by Different Sol-Gel Route. Acta Phy Polonica A, 118: 659-664.

Ilıcan S, Caglar Y, Caglar M. 2008. Preparation and characterization of ZnO thin films deposited by sol-gel spin coating method. J Optoelect Adv Mat, 10: 2578-2583.

Iribarren A, Fernández P, Piqueras J. 2008a. Cathodoluminescence characterization of ZnO:Te microstructures obtained with ZnTe and TeO2 doping precursors. Superlattices and Microstructures, 43: 600-604.

Iribarren A, Fernández P, Piqueras J. 2008b. Cathodoluminescence study of Te-doped ZnO microstructures grown by a vapour–solid process. J Mater Sci, 43: 2844-2848.

Iribarren A, Fernández P, Piqueras J. 2009a. Influence of defects on cathodoluminescence along ZnTex01-x–ZnO microstructures grown by the vapour-solid technique. Rev Cub Física, 26: 116-119.

Iribarren A, Fernández P, Piqueras J. 2009b. TeO2-doped ZnO micro and nanostructures grown by the vapour–solid technique. Rev Cub Física, 26: 42-46.

Jiang M, Liu X, Wang H. 2009. Optical emission spectra of Zn and Bi in pulsed magnetron plasma. Surf Coat Tech, 203: 3750-3753.

Karthikeyan B, Sandeep C S S, Philip R, Baesso M L. 2009. Study of optical properties and effective three-photon absorption in Bi-doped ZnO nanoparticles. J Appl Phys, 106: 114304 - 114305.

Lee J H, Ko K H, Park B O. 2003. Electrical and Optical Properties of ZnO Transparent Conducting Films by the Sol–Gel Method. J Cryst Growth, 247: 119-125.

Lee J. W, Subramaniam N G, Lee J C S, Kang T W. 2011. Study of stable p-type conductivity in bismuth-doped ZnO films grown by pulsed-laser deposition. A letters J Explor Front Phys (EPL), 95: 47002.

Maksimov O. 2010. Recent advances and novel approaches of p-type doping of zinc oxide. Rev Adv Mater Sci, 24: 26-34.

Merita S, Krämer T, Mogwitz B, Franz B, Polity A, Meyer B K. 2004. Oxygen in sputter-deposited ZnTe thin films. Phys Stat Sol (c), 3: 960-963.

Meulenkamp E A. 1999. Electron Transport in Nanoparticulate ZnO Films. J Phys Chem B, 103: 7931.

Pan H L, Yao B, Ding M, Deng R, Yang T, Sui Y R, Gao L L. 2010. Characterization and properties of Zn–O–Se ternary system thin films deposited by radio-frequency (rf)-magnetron sputtering. J Non-Cryst Sol, 356: 906-910.

Park S, Minegishi T, Oh D, Lee H, Taishi T, Park J, Yao T. 2010. High-Quality p-Type ZnO Films Grown by Co-Doping of N and Te on Zn-Face ZnO Substrates. Appl Phys Expr, 3: 031103.

Park S H, Minegishi T, Lee H J, Park J S, Im I H, Yao T, Chang J H. 2010. Investigation of the crystallinity of N and Te codoped Zn-polar ZnO films grown by plasma-assisted molecular-beam epitaxy. J Appl Phys, 108: 093518

Pawar B N, Ham D H, Mane R S, Ganesh T, Cho B W, Han S H. 2008. Fluorine-doped zinc oxide transparent and conducting electrode by chemical spray synthesis. Appl Surf Sci, 254: 6294-6297.

Porter H L, Muth J F. 2006. Photoluminescence study of ZnO films codoped with nitrogen and tellurium. J Appl Phys, 100: 123102.

Ravichandran K, Muruganantham G, Sakthivel B. 2009. Highly

conducting and crystalline doubly doped tin oxide films fabricated using a low-cost and simplified spray technique. Physica B, 404: 4299-4302.

Roknabadi M R, Behdani M, Arabshahi H, Hodeini N. 2009. Influence of hydrogen plasma on properties of transparent PEDT/PSS thin films. Int Rev Phy, 12: 153-157.

Sagar P, Kumar M, Mehra R M. 2005. Electrical and optical properties of sol-gel derived ZnO:Al thin films. Mater Sci-Poland, 23: 685-696.

Sanchez-Juarez A, Tiburcio-Silver A, Ortizc A, Zironi E P, Rickards J. 1998. Electrical and optical properties of fluorine-doped ZnO thin films prepared by spray pyrolysis. Thin Solid Films, 333: 196-202.

Sargolzaei M, Lotfizadeh N, Hayn R. 2011. First principles study on magnetic properties of Zn vacancies in ZnO doped with single chalcogen X (X= S, Se, and Te). J Appl Phys, 109: 073705.

Scherrer P, Nachrichten G. 1918. Effect of Carbon Fillers in Ultrahigh Molecular Weight Polyethylene Matrix Prepared by Twin-Screw Extrusion. Math Phys, 2: 98-100.

Serin T, Serin N, Karadeniz S, Sarı H, Tuğluoğlu N, Pakma O. 2006. Electrical, structural and optical properties of SnO2 thin films prepared by spray pyrolysis. J Non-Cryst Sol, 352: 209–215.

Tang K, Gu S, Wu K, Zhu S, Ye J, Zhang R, Zheng Y. 2010. Tellurium assisted realization of p-type N-doped ZnO. Appl Phys Lett, 96: 242101.

Tauc J, Grigorovici R, Vancu A. 1966. Optical Properties and Electronic Structure of Amorphous Germanium. Phys Status Solidi (b), 15: 627-637.

Tilley R J D. 2006. Crystal and Crystal structures. Wiley, London, UK.

Wenckstern H V, Schmidt H, Brandt M, Lajn A, Pickenhain R, Lorenz M, Jug K. 2009. Anionic and cationic substitution in ZnO. Prog Sol State Chem, 37: 153-172.